Supplementary Information: Cell-specific Bioorthogonal Tagging of Glycoproteins

B. Schumann *et al.*

Supplementary Figures

Supplementary Methods

Anna Cioce[1,2], Beatriz Calle[1,2,3], Tatiana Rizou[3,$], Sarah C. Lowery[4,$], Victoria L. Bridgeman[3,$], Keira E. Mahoney[4,$], Andrea Marchesi[1,2], Ganka Bineva-Todd[2], Helen Flynn[5], Zhen Li[1,2], Omur Y. Tastan[2], Chloe Roustan[6], Pablo Soro-Barrio[7], Mahmoud-Reza Rafiee[8], Acely Garza-Garcia[9], Aristotelis Antonopoulos[10], Thomas M. Wood[11,14], Tessa Keenan[12], Peter Both[13,15], Kun Huang[13,16], Fabio Parmeggian[13,17], Ambrosius P. Snijders[5], Mark Skehel[5], Svend Kjær[6], Martin A. Fascione[12], Carolyn R. Bertozzi[11], Stuart M. Haslam[10], Sabine L. Flitsch[13], Stacy A. Malaker[4], Ilaria Malanchi[3], Benjamin Schumann[1,2,*]

[1]Department of Chemistry, Imperial College London, W12 0BZ London, UK.

[2]Chemical Glycobiology Laboratory, The Francis Crick Institute, NW1 1AT London, UK.

[3]Tumour-Host Interaction Laboratory, The Francis Crick Institute, NW1 1AT London, UK.

[4]Department of Chemistry, Yale University, CT 06511 New Haven, USA.

[5]Proteomics Science Technology Platform, The Francis Crick Institute, NW1 1AT London, UK.

[6]Structural Biology Science Technology Platform, The Francis Crick Institute, NW1 1AT London, UK.

[7]Bioinformatics & Biostatistics Science Technology Platform, The Francis Crick Institute, NW1 1AT London, UK.

[8]RNA Networks Laboratory, The Francis Crick Institute, NW1 1AT London, UK.

[9]Mycobacterial Metabolism and Antibiotic Research Laboratory, The Francis Crick Institute, NW1 1AT London, UK.

[10]Department of Life Sciences, Imperial College London, SW7 2AZ London, UK.

[11]Sarafan ChEM-H, Department of Chemistry and Howard Hughes Medical Institute, Stanford University, CA 94305 Stanford, USA.

[12]Department of Chemistry, University of York, YO10 5DD York, UK.

[13]School of Chemistry & Institute of Biotechnology, The University of Manchester, M1 7DN Manchester, UK.
[14]current address: Massachusetts Institute of Technology, MA 02139 Cambridge, USA.
[15]current address: R&D Department, Axxence Slovakia s.r.o., 81107 Bratislava, Slovakia
[16]current address: Department of Chemistry and Biochemistry, University of Maryland, MD 20742 College Park, USA.
[17]current address: Department of Chemistry, Materials and Chemical Engineering "G. Natta", Politecnico di Milano, 20131 Milano, Italy
[$]These authors contributed equally.
*Correspondence should be addressed to: b.schumann@imperial.ac.uk.

Supplementary Figures

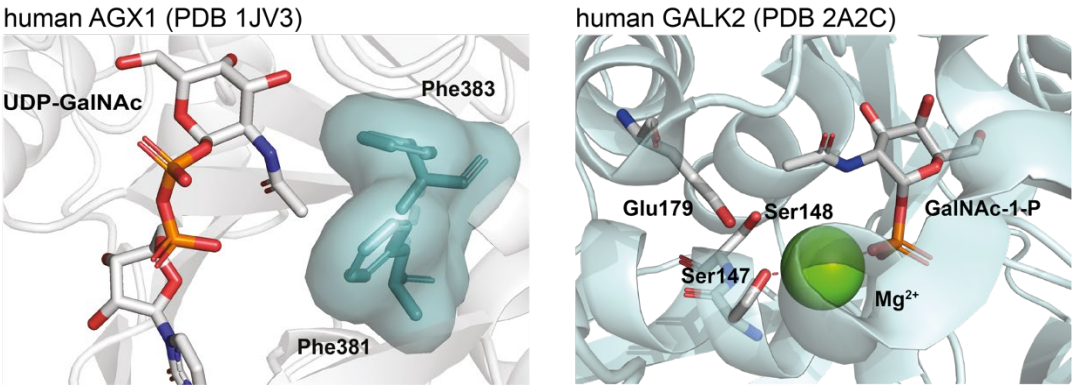

Supplementary Figure 1: Active site architectures of human enzymes of the GalNAc salvage pathway. In AGX1, the *N*-acyl side chain in UDP-GalNAc is in proximity to Phe381 and Phe383. In GALK2, the *N*-acyl side chain of GalNAc-1-phosphate is in proximity to the peptide backbone and amino acids forming a hydrogen network (Glu179, Ser147 and Ser148). Structures are modelled based on protein databank acquisition numbers 1JV3[1] and 2A2C.[2]

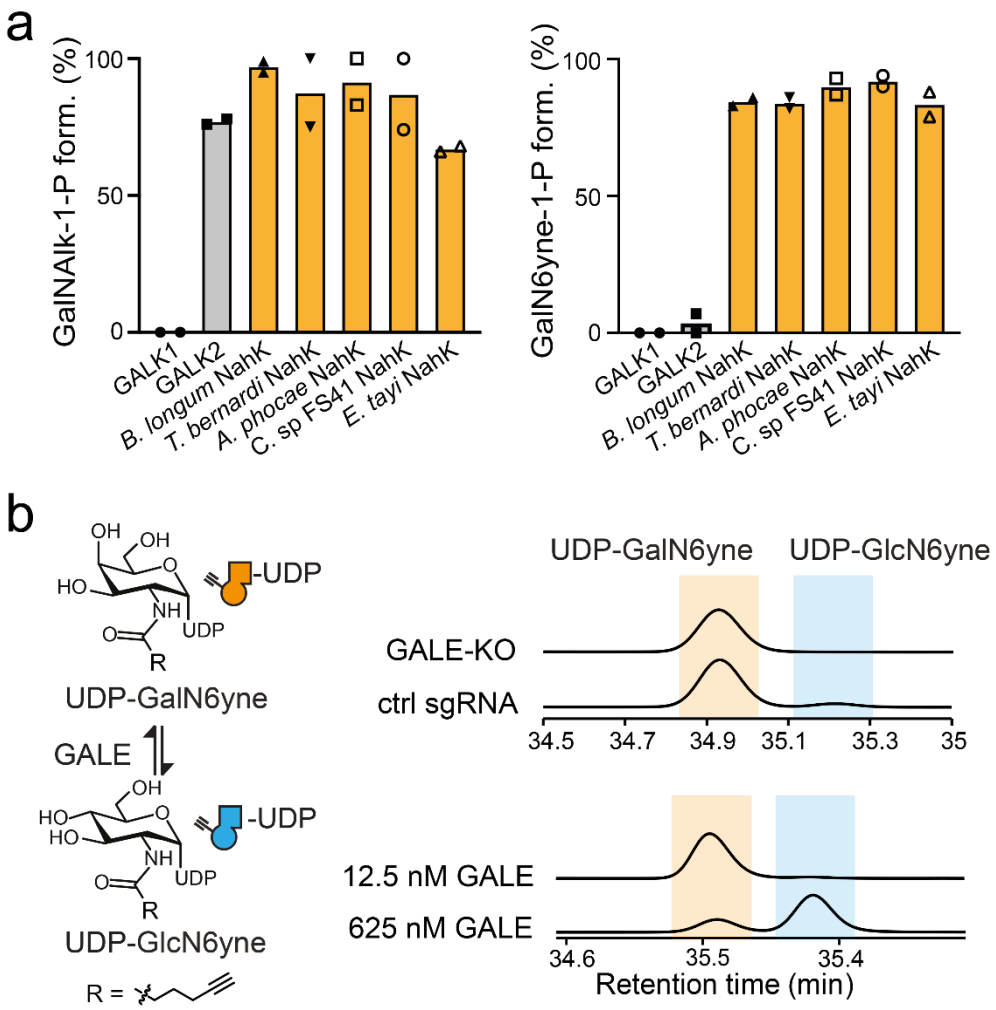

Supplementary Figure 2: Evaluation of enzymatic turnover of GalN6yne-based metabolites. a, *in vitro* GalN6yne-1-phosphate and GalNAlk-1-phosphate formation by human and bacterial GalNAc kinases, as assessed by Liquid Chromatography-Mass Spectrometry (LC-MS) and integrated ion count. Data are individual data points and means from two individual experiments. **b,** ion pair HPLC traces of *in vitro* epimerisation assays, using UDP-GalN6yne as substrate and either cell lysates from control or GALE-KO K-562 cells or two different concentrations of purified GALE as enzyme sources.[3] Data are representative of two independent replicates (lysate samples) or from one experiment (isolated GALE samples). Traces depict relative intensity of absorbance at 260 nm. Source data are provided as a Source Data file.

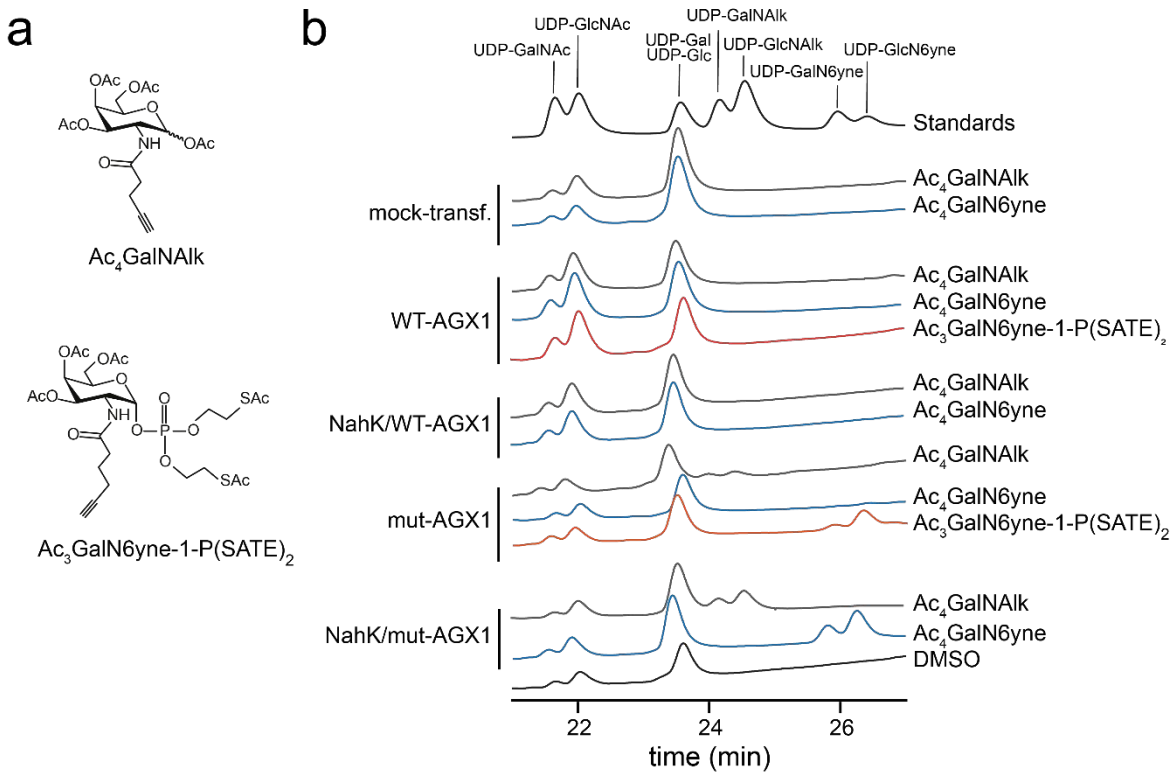

Supplementary Figure 3: Biosynthesis of chemically tagged UDP-sugars by metabolic engineering. a, structures of two MOE reagents used herein. $Ac_3GalN6yne\text{-}1\text{-}P(SATE)_2$ is a caged precursor of GalN6yne-1-phosphate. **b,** biosynthesis of UDP-sugars in cells mock or stably transfected with metabolic enzymes, as assessed by High Performance Anion Exchange Chromatography (HPAEC). Retention times were normalised on an external standards. Synthetic UDP-sugars served as standards. Data are from one representative out of two independent experiments performed on two different days. Source data are provided as a Source Data file.

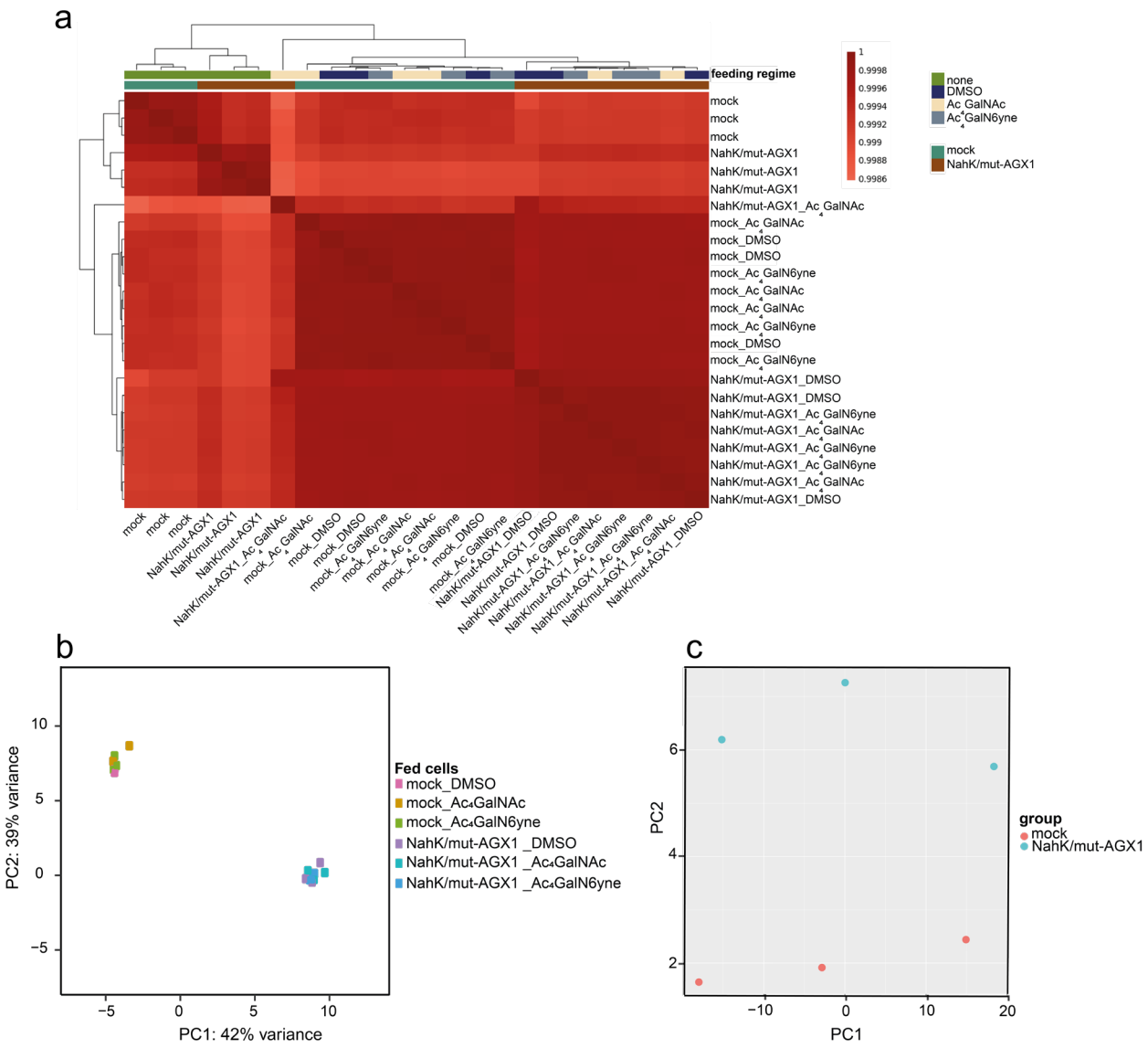

Supplementary Figure 4: Transcriptomic analysis of K-562 cells at different transfection conditions and feeding regimes. RNAs were extracted from K-562 cells transfected with either pSBbi-GH (mock) or pSBbi-NahK/mut-AGX1 at different feeding regimes (either unfed, DMSO, 10 µM Ac_4GalNAc or 10 µM Ac_4GalN6yne). **a,** Correlation plot and **b,** Principal component analysis (PCA) plot of transfected K-562 cells at different feeding regimes. Data are from one representative out of a total of three replicates collected on the same day. **c,** Previous experiment performed on RNA extracted from K-562 cells, transfected with either pSBbi-GH (mock) or pSBbi-NahK/mut-AGX1, showed significant variation in PCA associated with the different day of collection.

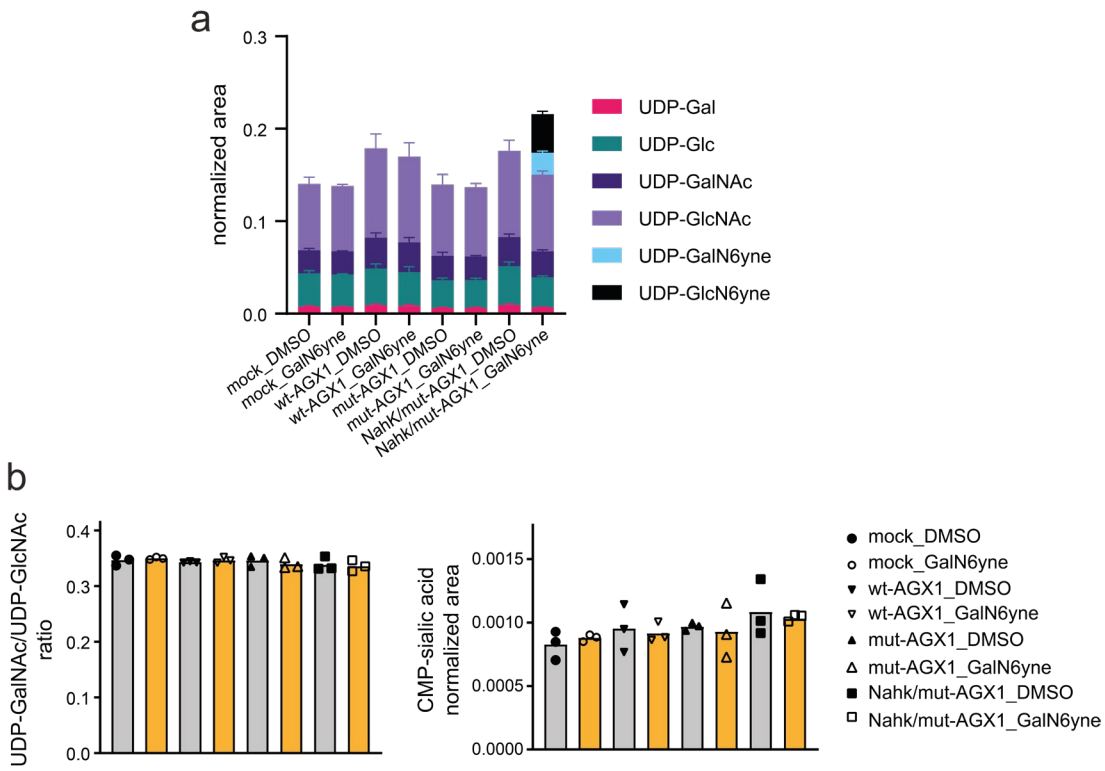

Supplementary Figure 5: Quantification of UDP-sugars assessed by High Performance Ion-pair Reversed-Phase Chromatography (IP RP HPLC). a, total amount of UDP-Hex, UDP-HexNAc and modified UDP-HexNAc in pSBbi-transfected K-562 cells fed with either 10 µM Ac_4GalN6yne or DMSO. Data are from three biological replicates, collected on the same day, depicted as means + standard deviation (SD). **b,** UDP-GalNAc/UDP-GlcNAc ratio and CMP-sialic acid levels across the different K-562 cell lines and feeding regimes. Data are from three biological replicates, collected on the same day, depicted as individual data points and means. UDP-sugar areas were normalised against the total area between 0 and 65 min. Source data are provided as a Source Data file.

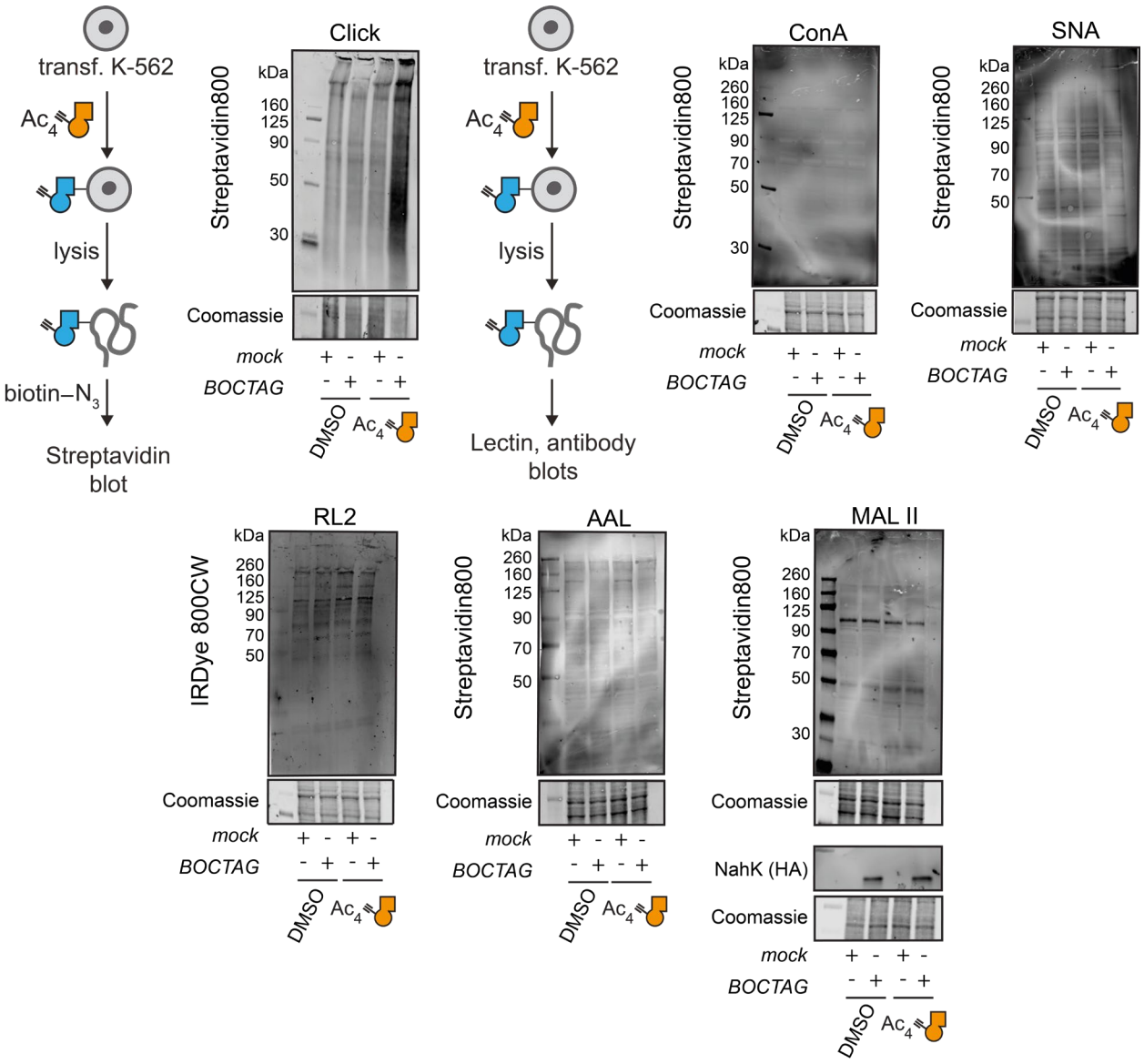

Supplementary Figure 6: Lectin and immunoblot analyses: BOCTAG and mock-transfected K-562 cells. Evaluation of whole lysate tagging and glycoproteins profile after treating K-562 stably expressing NahK/mut-AGX1 or an empty plasmid with either 10 µM Ac_4GalN6yne or DMSO. Data are from one experiment. ConA: Concanavalin A; AAL: Aleuria Aurantia Mushrooms; MAL II: Maackis Amurensis II, SNA: Sambucus Nigra; RL2: O-GlcNAc Antibody. Source data are provided as a Source Data file.

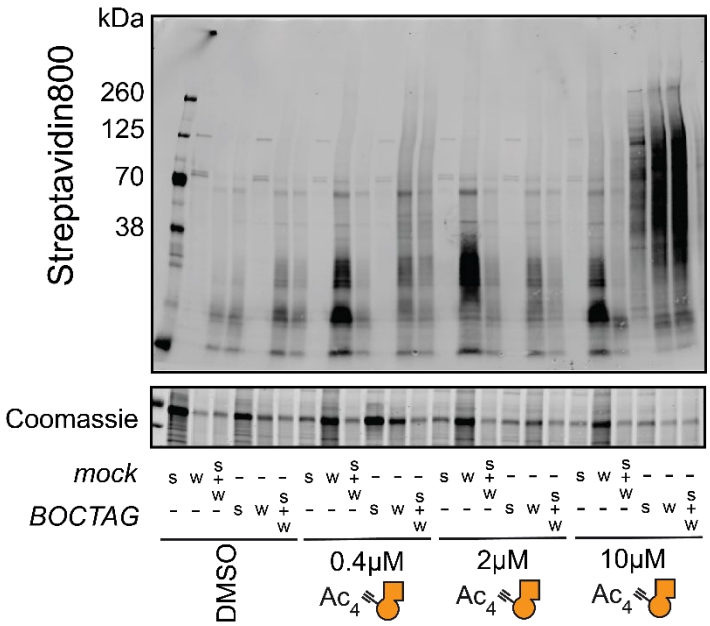

Supplementary Figure 7: Evaluation of chemical tag incorporation on cell surface, in cell lysate or both by feeding mock- and NahK/mut-AGX1-transfected K-562 cells with either different concentrations of Ac_4GalN6yne or DMSO. Glycoproteins were visualised by streptavidin blot after treating cells with biotin-picolyl azide under CuAAC conditions followed by streptavidin blot. Cell surface labelling was performed prior to cell lysis while whole lysate labelling was performed after lysis.

s: cell surface labelling, w: whole lysate labelling, s+w: cell surface and whole lysate labelling. Data are from one experiment. Source data are provided as a Source Data file.

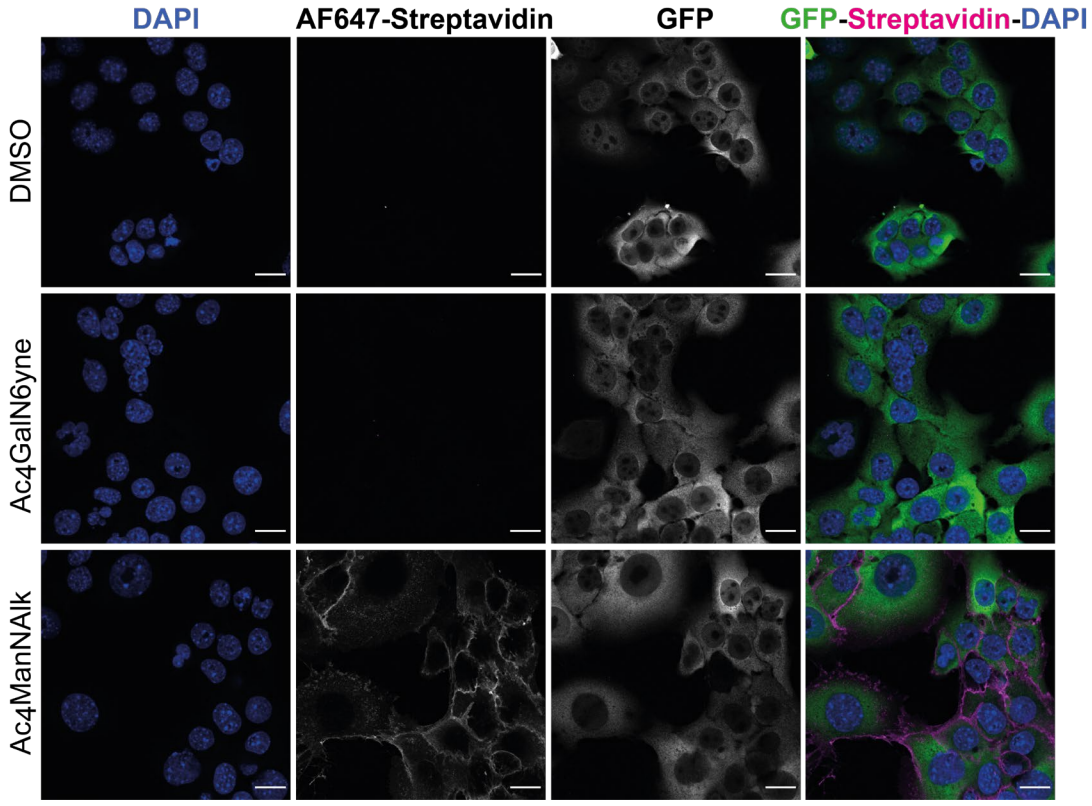

Supplementary Figure 8: Fluorescence microscopy of GFP-expressing 4T1 cells, transfected with empty plasmid pSBbi-Hyg, fed overnight with either DMSO, 50 µM Ac_4GalN6yne or 50 µM Ac_4ManNAlk, treated with biotin-picolyl azide under CuAAC conditions and visualised with AlexaFluor647-Streptavidin. Scale bar, 20 µm. Data are representative of two independent experiments.

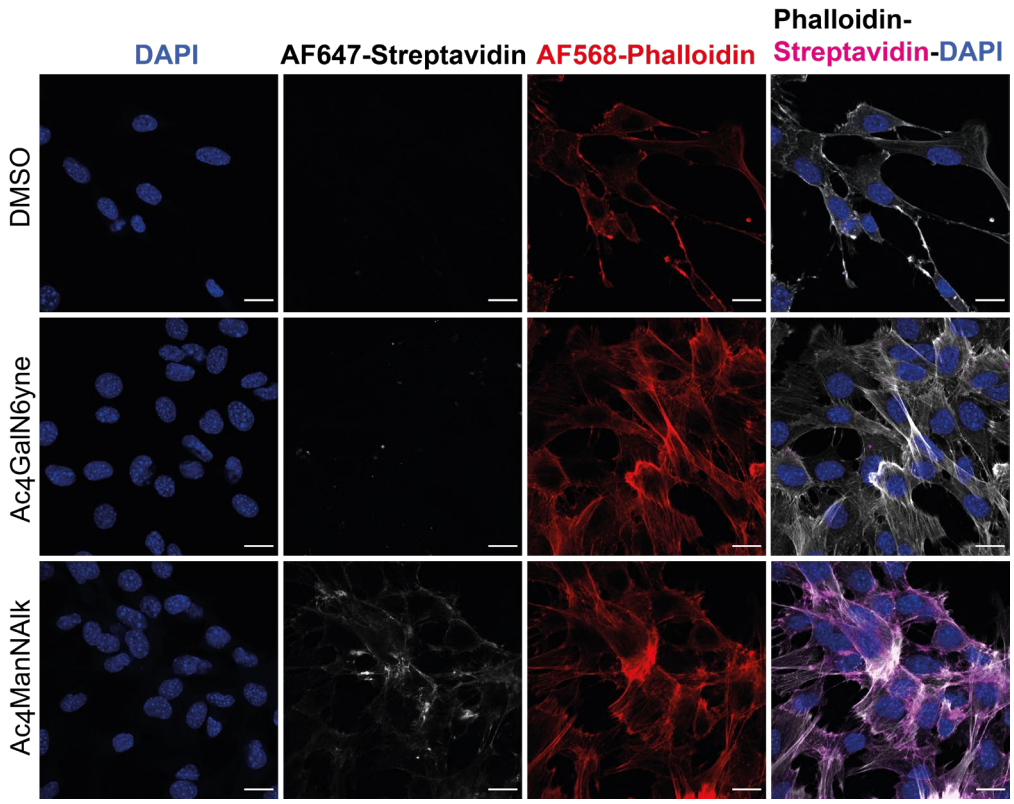

Supplementary Figure 9: Fluorescence microscopy of non-transfected MLg cells fed overnight with DMSO, 50 µM Ac_4GalN6yne or 50 µM Ac_4ManNAlk treated with biotin-picolyl azide under CuAAC conditions and visualised with AlexaFluor647-Streptavidin. Scale bar, 20 µm. Data are representative of two independent experiments.

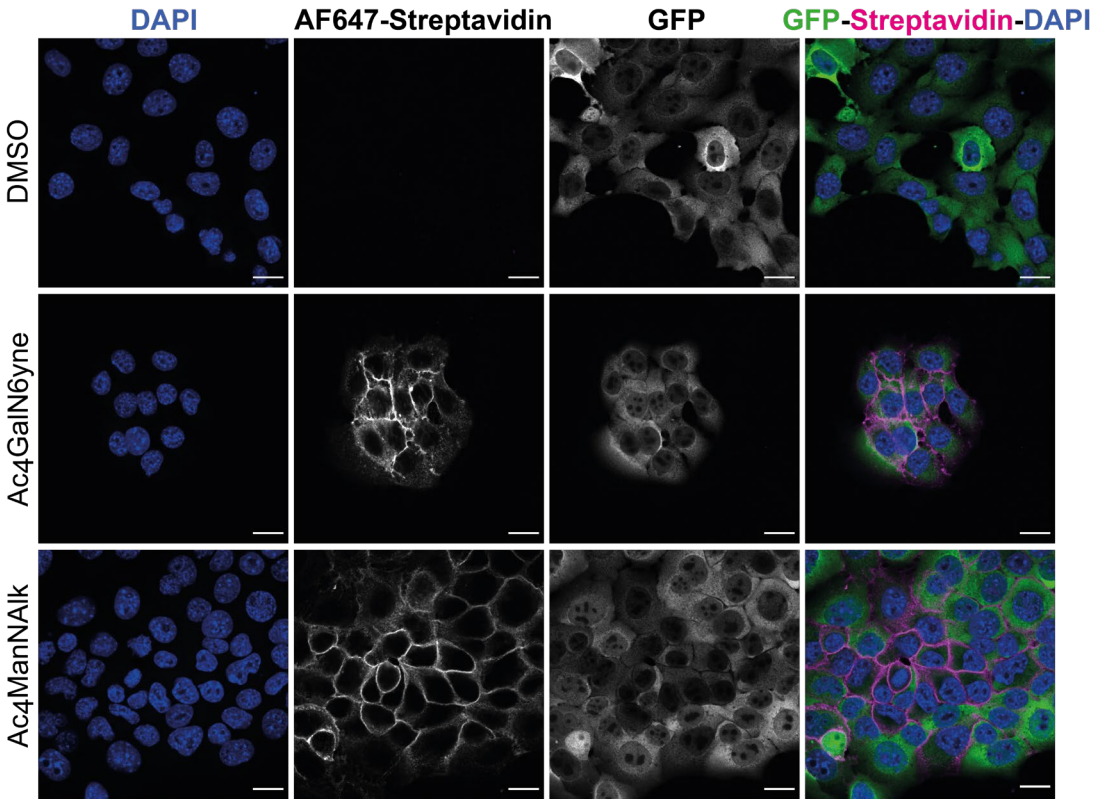

Supplementary Figure 10: Fluorescence microscopy of GFP-expressing 4T1 cells, transfected with pSBbi-NahK/mut-AGX1, fed overnight with either 50 µM Ac_4GalN6yne or 50 µM Ac_4ManNAlk treated with biotin-picolyl azide under CuAAC conditions and visualised with AlexaFluor647-Streptavidin. Scale bar, 20 µm. Data are representative of two independent experiments.

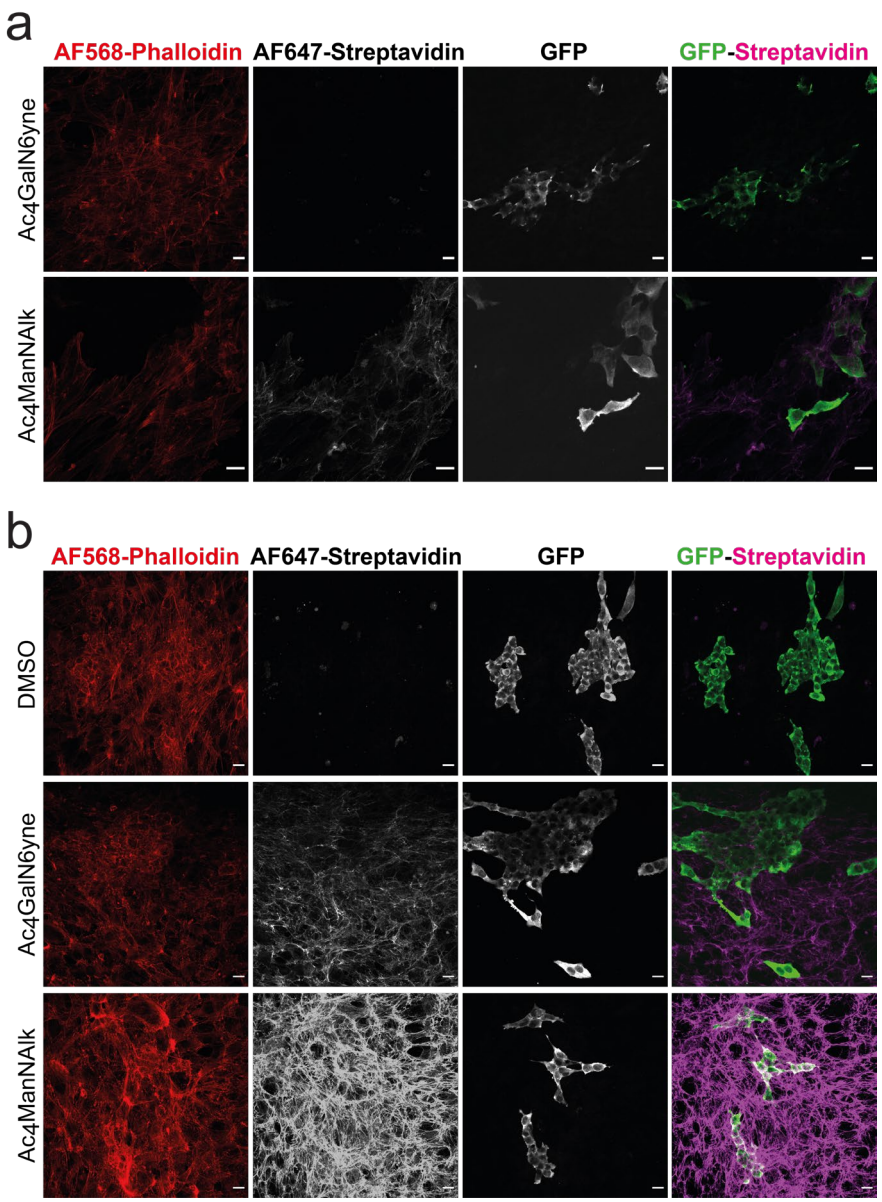

Supplementary Figure 11: Maximum intensity projection from a z-stack acquisition of **a,** GFP-expressing 4T1 and MLg cells, both transfected with pSBbi-Hyg empty plasmid, in a co-culture system fed overnight with either 50 µM Ac_4GalN6yne or 50 µM Ac_4ManNAlk. **b,** GFP-expressing 4T1 and MLg cells, both transfected with pSBbi-NahK/mut-AGX1 plasmid, in a co-culture system fed overnight with either DMSO, 50 µM Ac_4GalN6yne or 50 µM Ac_4ManNAlk. Co-culture samples in both a and b were treated with biotin-picolyl azide under CuAAC conditions and visualised by AlexaFluor647-Streptavidin. Scale bar, 20 µm. Data are representative of two independent experiments.

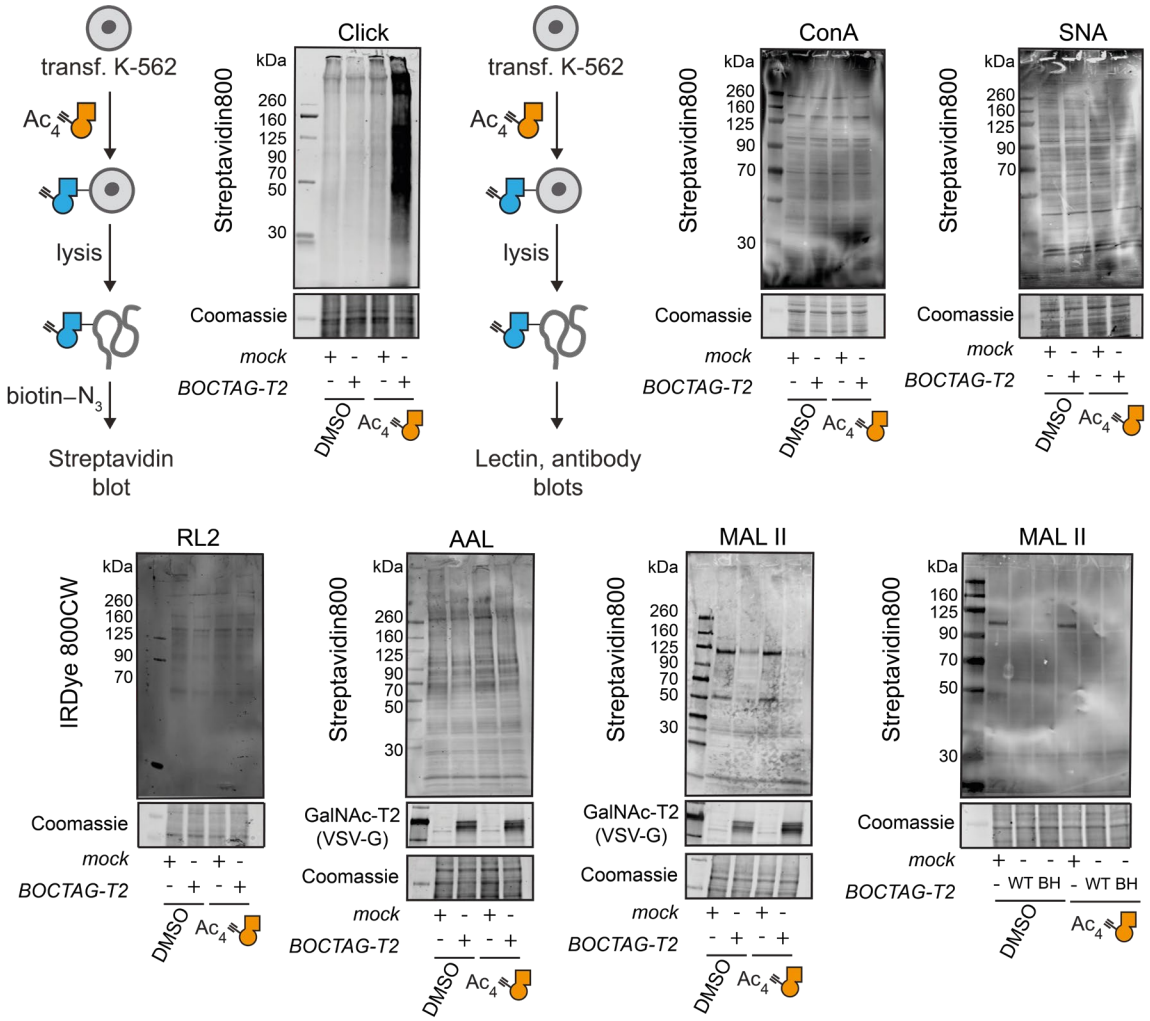

Supplementary Figure 12: Lectin and immunoblot analyses: BOCTAG-T2 and mock-transfected K-562 cells. Evaluation of whole lysate tagging and glycoproteins profile after treating K-562 stably expressing NahK/mut-AGX1/BH-T2 or an empty plasmid with either 10 µM Ac_4GalN6yne or DMSO. ConA: Concanavalin A; AAL: Aleuria Aurantia Mushrooms; MAL II: Maackis Amurensis II, SNA: Sambucus Nigra; RL2: O-GlcNAc Antibody. Data are from one experiment. Source data are provided as a Source Data file.

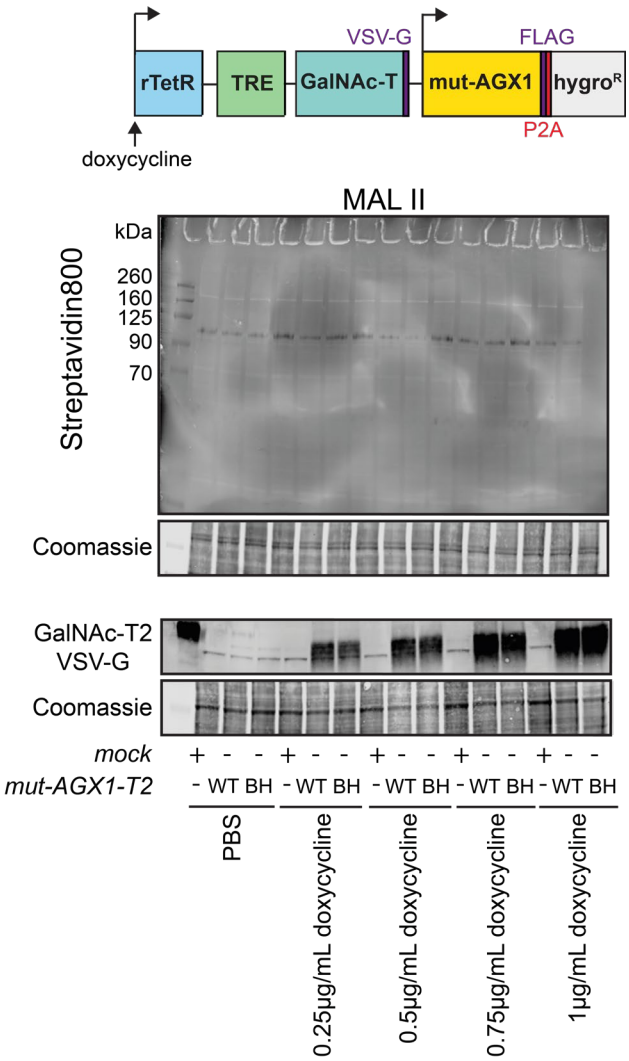

Supplementary Figure 13: MAL II binding at different WT- or BH-GalNAc-T2 expression levels. Cloning WT- or BH-GalNAc-T2 in a plasmid with a tetracycline-dependent promoter (pSBtet) allows to induce and modulate the expression levels of those enzymes in presence of tetracycline or one of its analogues like doxycycline. MAL II blot shows a change in the binding profile between mock- and mut-AGX1-T2 by increasing the expression levels of GalNAc-T2 (for both WT- and BH-GalNAc-T2 enzymes). Dose-response of WT- or BH-GalNAc-T2 expression is evaluated by anti-VSV-G staining. Data are from one experiment. Source data are provided as a Source Data file.

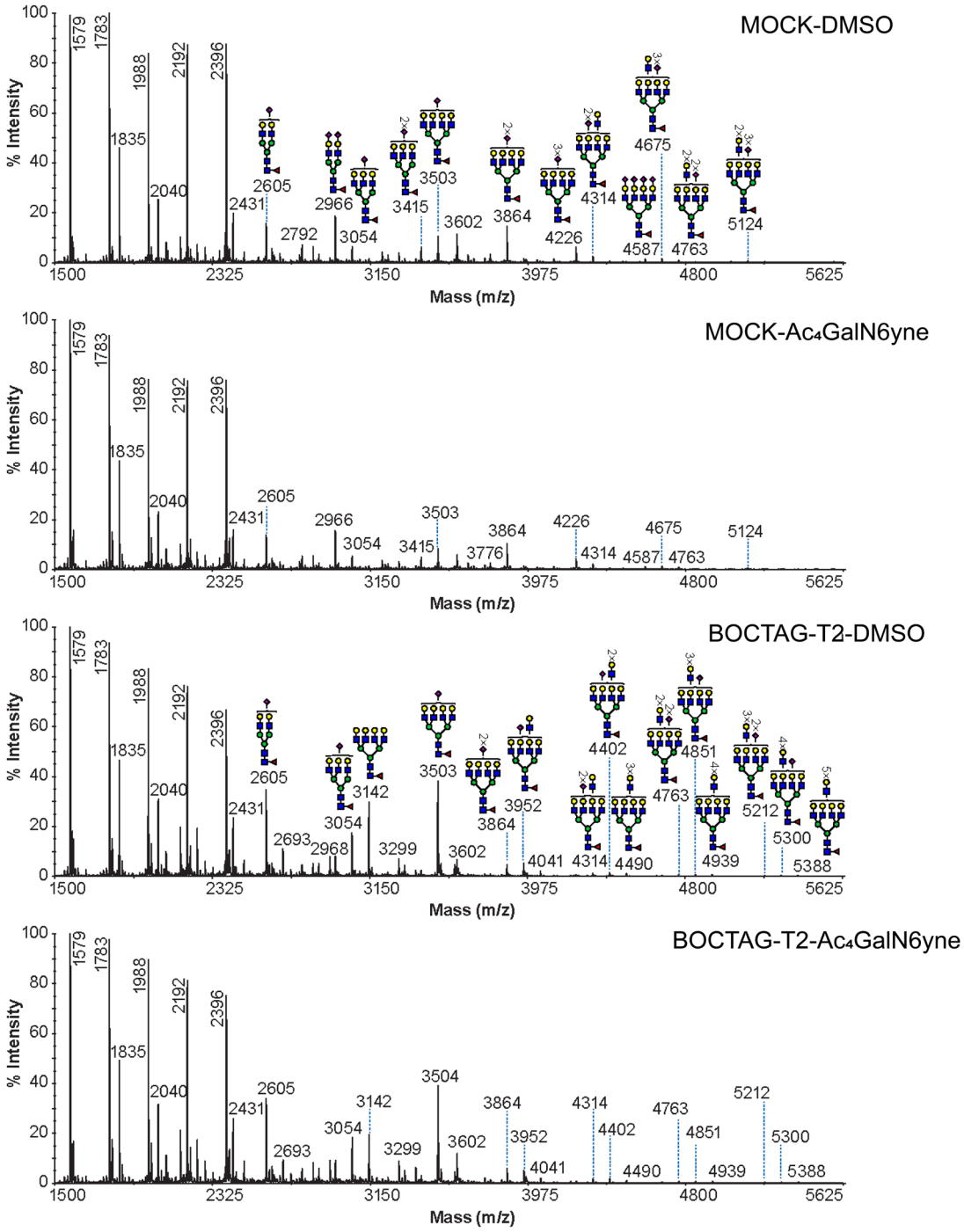

Supplementary Figure 14: Overall N-glycan structural analysis of K-562 cells transfected with mock or NahK/mut-AGX1-BH-GalNAc-T2 plasmids treated with either 10µM Ac_4GalN6yne or DMSO. N-glycans were released by peptide N-glycosidase F digestion, permethylated and analysed by MALDI-TOF/TOF. Data are from one experiment.

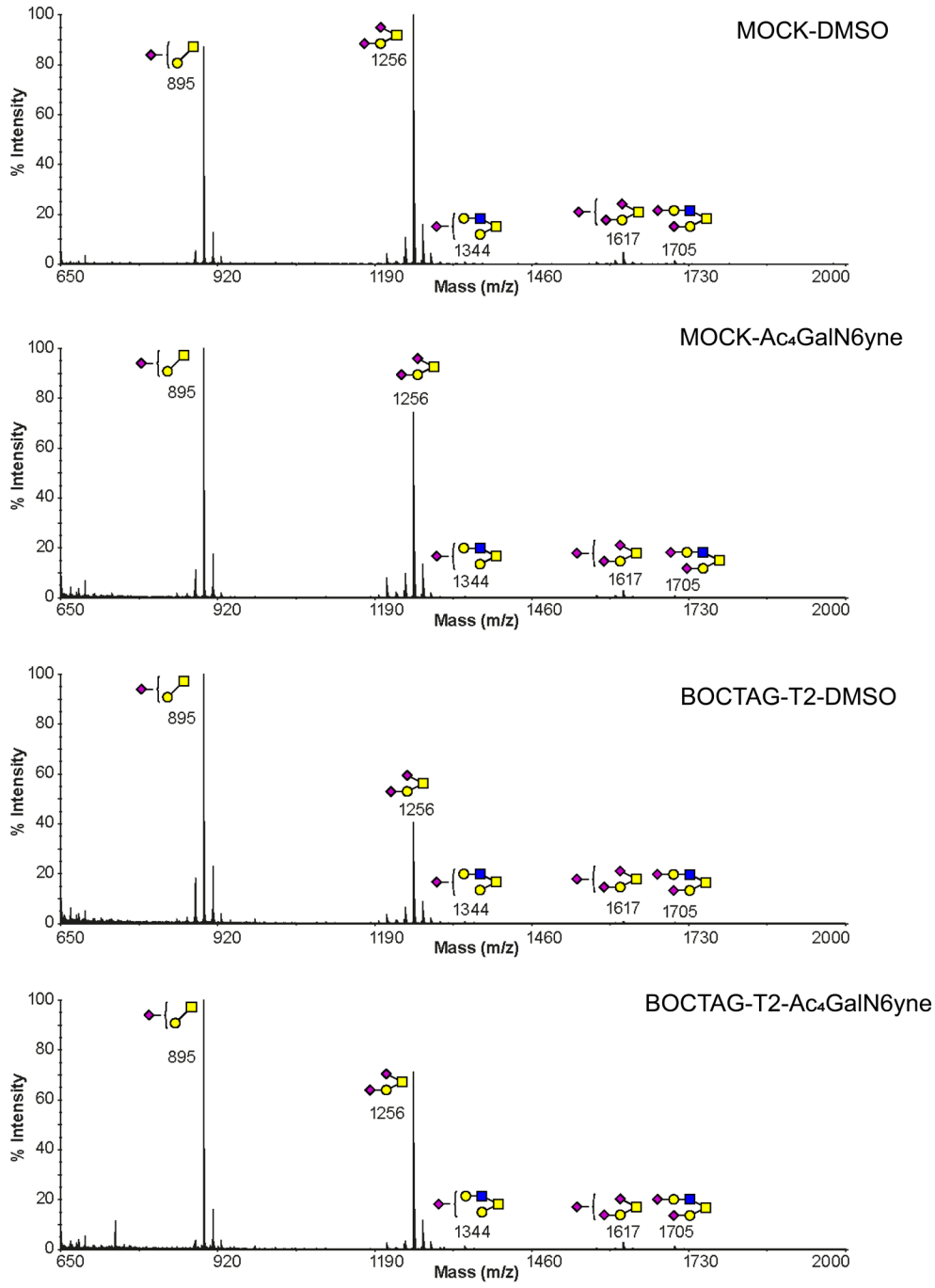

Supplementary Figure 15: Overall O-glycan structural analysis of K-562 cells transfected with mock- or NahK/mut-AGX1-BH-GalNAc-T2 plasmids treated with either 10µM Ac_4GalN6yne or DMSO. Data are from one experiment. O-glycans were released by reductive elimination, permethylated and analysed by MALDI-TOF/TOF. Data are from one experiment.

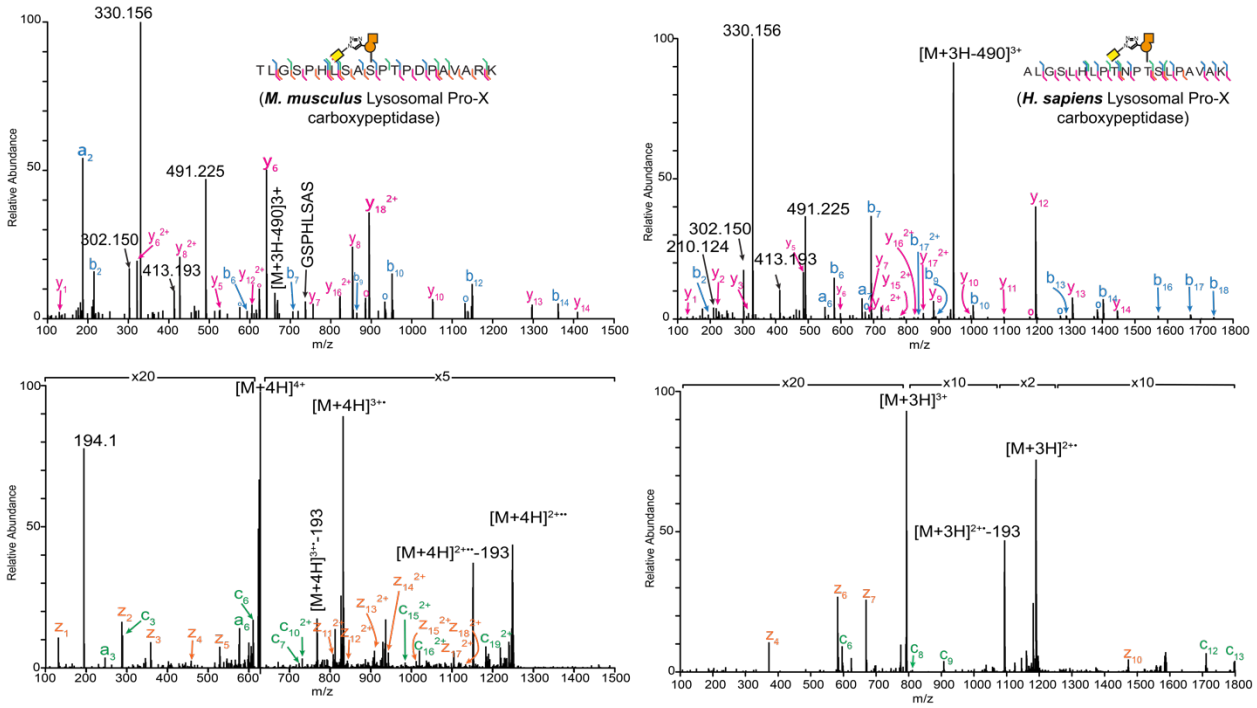

Supplementary Figure 16. Higher-energy Collisional Dissociation (HCD) and Electron Transfer Dissociation (ETD) spectra of homologous glycopeptides from murine (left) and human (right) origins enriched in secretome (**Fig. 5**).

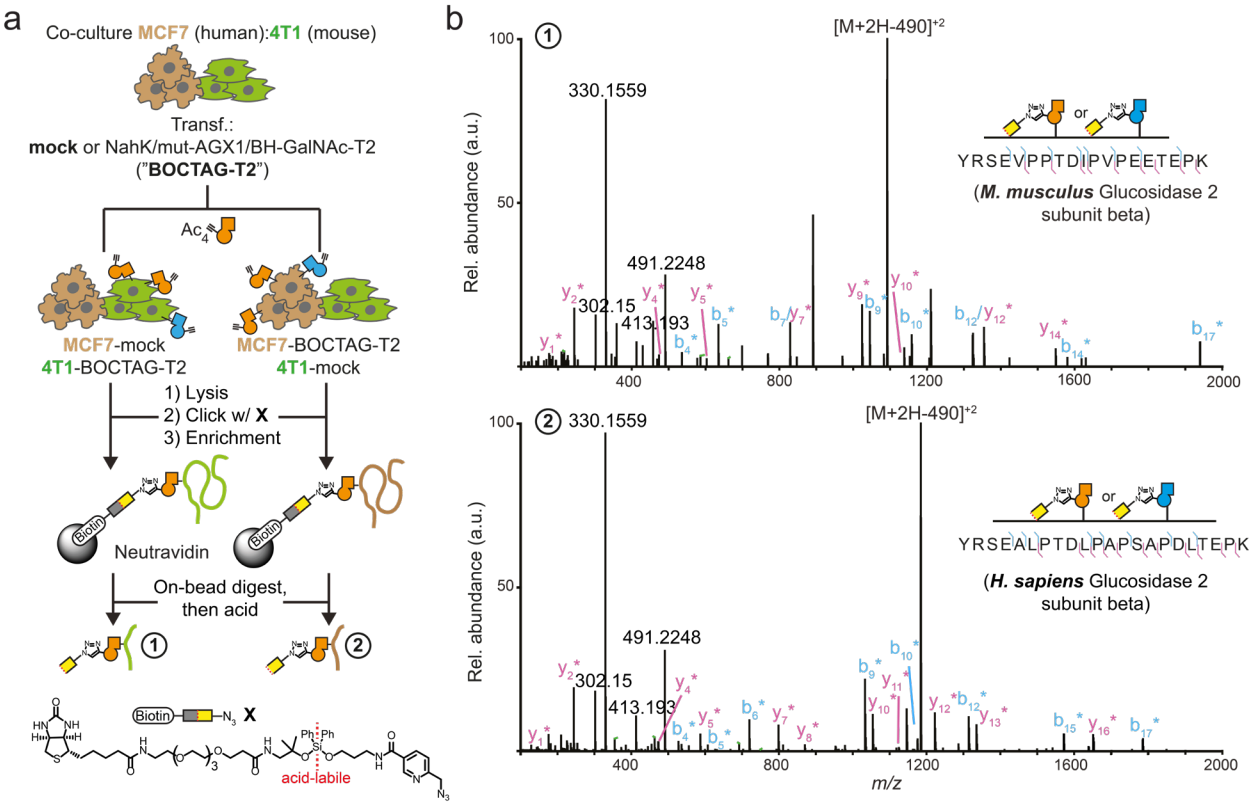

Supplementary Figure 17: Glycoproteomic analysis of lysates of co-cultured human and murine samples. a, cell-selective enrichment and MS-glycoproteomics of murine-human co-culture systems. MCF7 and 4T1 cells transfected as indicated were co-cultured overnight and treated with DMSO or 10 μM Ac_4GalN6yne for 24h. Lysates were subjected to CuAAC with acid-cleavable biotin-picolyl azide **X** and enriched on neutravidin beads. On-bead digest yielded peptide fractions while acid treatment of beads yielded glycopeptide fractions. **b,** Higher-energy Collisional Dissociation (HCD) spectra of homologous glycopeptides from murine (top) and human (bottom) origins.

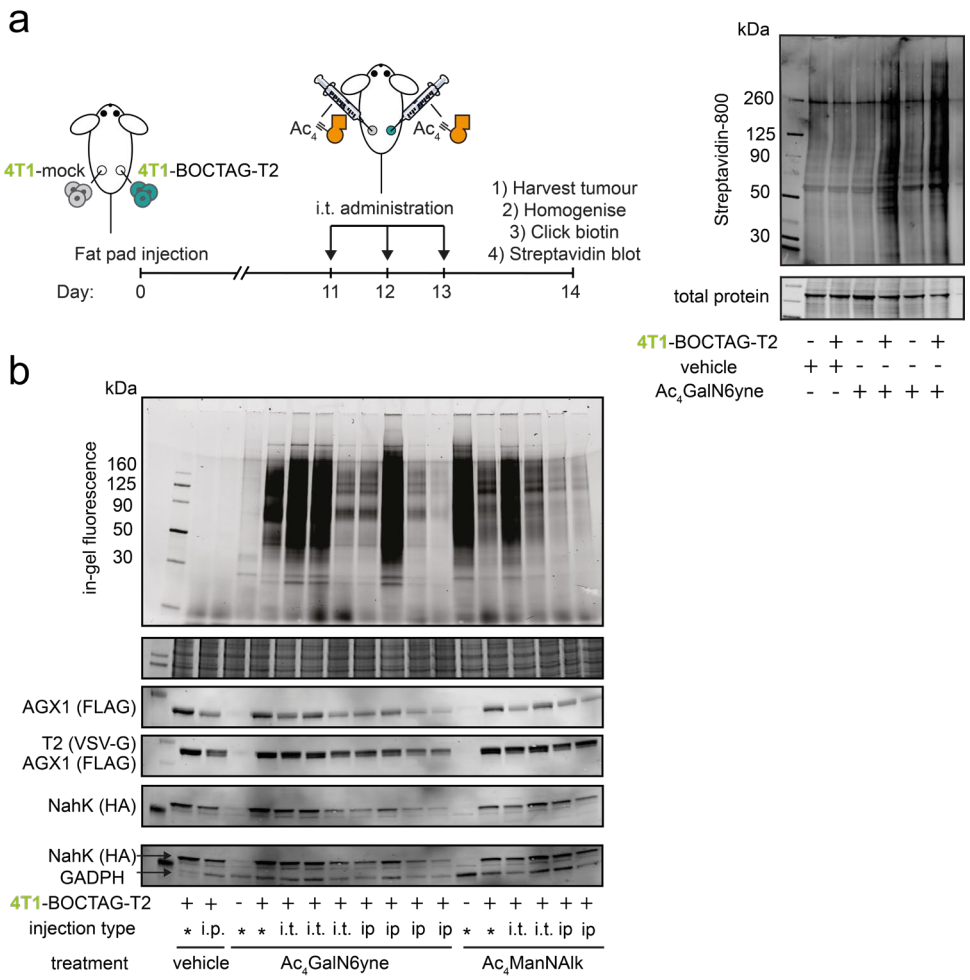

Supplementary Figure 18: BOCTAG labels glycoproteins in a cell-specific manner *in vivo*. **a,** BOCTAG-T2 and mock tumours were grown in the same mouse treated systemically for three days with 15 mg/kg Ac_4GalN6yne (n=2) or the corresponding volume of vehicle (5% (v/v) DMSO/ PEG-400, n=1) by intratumoral (i.t.) injection. Tumours were harvested, lysed, subjected to CuAAC with biotin-picolyl azide and analysed by streptavidin blot. **b,** after the experiment in **Fig.5** and **Supplementary Figure 18a**, BOCTAG-T2 cells were collected from intratumoral (i.t.) and intraperitoneal (i.p.) treated tumours, plated for 10 days in DMEM growing media and fed with either DMSO, Ac_4GalN6yne or Ac_4ManNAlk. Cell surface glycoprotein labelling efficiency of primary cells was validated by CuAAC with CF680-picolyl azide. Western blot was performed to assess levels of expression of BOCTAG-T2 enzymes. i.p.= intraperitoneal injection, i.t.= intratumoral injection, * = parental 4T1-mock and 4T1-BOCTAG-T2 cell lines. Data is representative of two independent experiments. Source data are provided as a Source Data file.

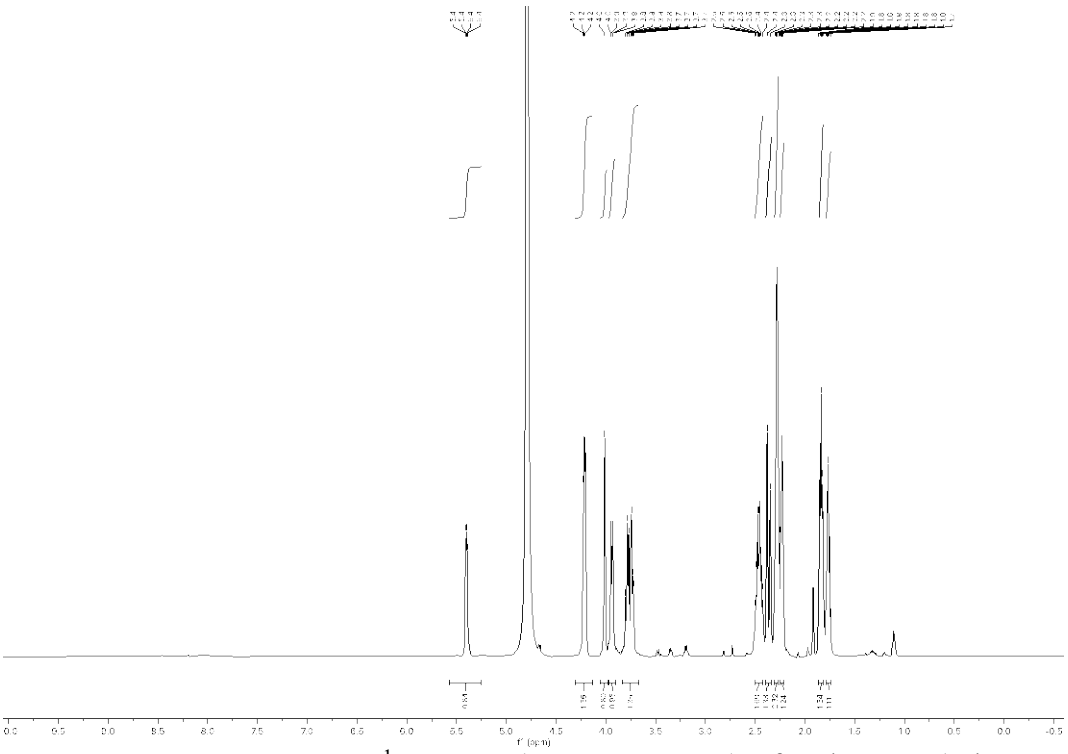

Supplementary Figure 19. ^{1}H NMR (600 MHz, D_2O) of 2-deoxy-2-(5-hexynoyl)amido-α-D-galactopyranosyl phosphate disodium salt **SI-3**

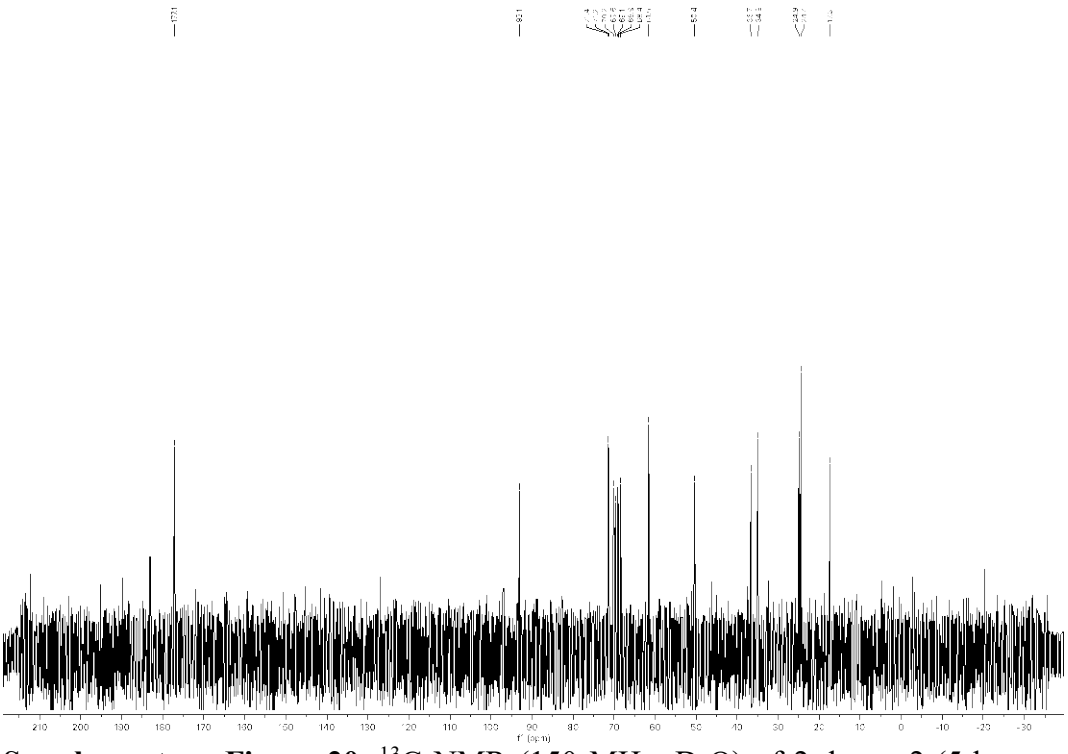

Supplementary Figure 20. ^{13}C NMR (150 MHz, D_2O) of 2-deoxy-2-(5-hexynoyl)amido-α-D-galactopyranosyl phosphate disodium salt **SI-3**

Supplementary Methods

Chemical synthesis

2-deoxy-2-(5-hexynoyl)amido-α-D-galactopyranosyl phosphate disodium salt (SI-3)

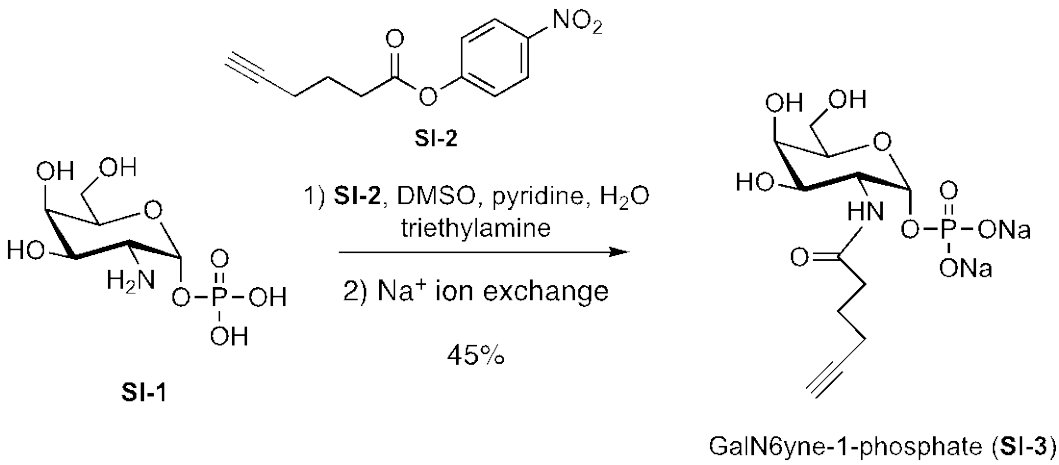

Commercial amine **SI-1** (15 mg, 58 µmol) in anhydrous DMSO/pyridine (1:1.5 (v/v), 1.2 mL) was treated with 4-nitrophenyl hex-5-ynoate **SI-2** (20 mg, 87 µmol) and triethylamine (8 µL, 58 µmol). The turbid solution was left to stir overnight. The reaction was treated with 100 µL water and left to stir for another 8 h. Another 150 µL water were added as well as 1.5 equiv. reagent **SI-2** (20 mg, 87 µmol). After another 60 h, another 200 µL water were added, then another 1.5 equiv. reagent **SI-2** (20 mg, 87 µmol). The yellow solution turned clear overnight, when TLC (DCM/MeOH/water 4:1:1 with 2 drops triethylamine) indicated conversion. The solution was shock frozen on dry ice, lyophilised and purified by size exclusion chromatography (Sephadex G-25 extra fine, Sigma-Aldrich) using water/MeOH 3:2 (v/v) as a solvent. The combined fractions were concentrated and passed through AG 50W-X8 Na^+ form resin (Bio-Rad) and lyophilised to give alkyne **SI-3** (10 mg, 26 µmol, 45%) as a white solid. ^{1}H NMR (600 MHz, D_2O) δ 5.40 (dd, J = 7.5, 3.5 Hz, 1H), 4.31 – 4.14 (m, 2H), 4.01 (s, 1H), 3.94 (dd, J = 10.9, 3.1 Hz, 1H), 3.84 – 3.67 (m, 2H), 2.46 (m, J = 14.8, 7.2 Hz, 2H), 2.39 – 2.33 (m, 2H), 2.28 (m, 4H), 2.23 (m, 1H), 1.84 (m, 1H), 1.76 (m, 1H); ^{13}C NMR (150 MHz, D_2O) δ 177.1, 93.1, 71.4, 71.2, 70.2, 69.6, 69.1, 68.9, 68.4, 61.6, 50.4, 36.7, 34.9, 24.9, 24.4, 17.3; HRMS (m/z): $[M-H]^-$ calcd. for $C_{12}H_{20}NO_9P$, 352.0876; found, 352.0800.

Supplementary References

1. Pennef, C. *et al.* Crystal strucutre of two human pyrophosphorylase isoforms in complexes with UDPGlc(Gal)NAc: Role of the alternatively spliced insert in the enzyme oligomeric assembly and active site architecture. *EMBO J.* **20**, 6191–6202 (2001).
2. Thoden, J. B. & Holden, H. M. The molecular architecture of human N-acetylgalactosamine kinase. *J. Biol. Chem.* **280**, 32784-32791 (2005).
3. Debets, M. F. *et al.* Metabolic precision labeling enables selective probing of O-linked N-acetylgalactosamine glycosylation. *Proc. Natl. Acad. Sci.* **117**, 25293-25301 (2020).